Received: 11 August 2020 | Revised: 15 February 2021 | Accepted: 27 February 2021

DOI: 10.1002/pld3.315

ORIGINAL RESEARCH

# Root vacuolar sequestration and suberization are prominent responses of *Pistacia* spp. rootstocks during salinity stress

Shuxiao Zhang[1] | Alessandra Quartararo[1,2] | Oliver Karl Betz[1] | Shahab Madahhosseini[1] | Angelo Schuabb Heringer[1] | Thu Le[1] | Yuhang Shao[1] | Tiziano Caruso[2] | Louise Ferguson[1] | Judy Jernstedt[1] | Thomas Wilkop[1,3] | Georgia Drakakaki[1]

[1]Department of Plant Sciences, University of California Davis, Davis, CA, USA

[2]Department of Agricultural & Forest Science, University of Palermo, Viale delle Scienze, Palermo, Italy

[3]Light Microscopy Core, Department of Physiology, University of Kentucky, Lexington, KY, USA

**Correspondence**
Georgia Drakakaki, Department of Plant Sciences, University of California Davis, CA, USA.
Email: gdrakakaki@ucdavis.edu

**Present address**
Shahab Madahhosseini, Genetic and Plant Production Department, Vali-e-Asr University of Rafsanjan, Rafsanjan, Iran
Angelo Schuabb Heringer, Unidade de Biologia Integrativa, Setor de Genômica e Proteômica, UENF, Rio de Janeiro, RJ, Brazil
Yuhang Shao, Key Laboratory of Crop Physiology Ecology and Production Management of Ministry of Agriculture, Nanjing Agricultural University, Nanjing, Jiangsu Province, P. R. China

**Funding information**
This study was supported by the Pistachio Board of CA HC-2017-22, HC-2019-21 awards and the U.S. Department of Agriculture award CA-D-PLS-2132-H to G.D.

## Abstract

Understanding the mechanisms of stress tolerance in diverse species is needed to enhance crop performance under conditions such as high salinity. Plant roots, in particular in grafted agricultural crops, can function as a boundary against external stresses in order to maintain plant fitness. However, limited information exists for salinity stress responses of woody species and their rootstocks. Pistachio (*Pistacia* spp.) is a tree nut crop with relatively high salinity tolerance as well as high genetic heterogeneity. In this study, we used a microscopy-based approach to investigate the cellular and structural responses to salinity stress in the roots of two pistachio rootstocks, *Pistacia integerrima* (PGI) and a hybrid, *P. atlantica* x *P. integerrima* (UCB1). We analyzed root sections via fluorescence microscopy across a developmental gradient, defined by xylem development, for sodium localization and for cellular barrier differentiation via suberin deposition. Our cumulative data suggest that the salinity response in pistachio rootstock species is associated with both vacuolar sodium ion ($Na^+$) sequestration in the root cortex and increased suberin deposition at apoplastic barriers. Furthermore, both vacuolar sequestration and suberin deposition correlate with the root developmental gradient. We observed a higher rate of $Na^+$ vacuolar sequestration and reduced salt-induced leaf damage in UCB1 when compared to *P. integerrima*. In addition, UCB1 displayed higher basal levels of suberization, in both the exodermis and endodermis, compared to *P. integerrima*. This difference was enhanced after salinity stress. These cellular characteristics are phenotypes that can be taken into account during screening for sodium-mediated salinity tolerance in woody plant species.

KEYWORDS

endodermis, exodermis, pistachio rootstock, salinity tolerance, suberization, vacuolar sequestration

## 1 | INTRODUCTION

The combination of global climate change and dwindling freshwater supplies has increased the need for salt- and drought-tolerant crops. Among woody perennial nut crops, pistachio, a dioecious tree in the family Anacardiaceae, exhibits relatively high drought and salinity tolerance compared to other woody perennial crops (Ahmad & Prasad, 2012; Walker et al., 1987). Thus, pistachio emerged as a nut crop of increasing commercial interest both globally and in the USA (Ahmad & Prasad, 2012; Ferguson et al., 2002; Karimi et al., 2009). In laboratory and field conditions, the *Pistacia vera* scions, grown on several *Pistacia* spp. rootstocks, can tolerate sodium chloride (NaCl) concentrations of up to 150 mM (Ferguson et al., 2002; Walker et al., 1987). In contrast, citrus, avocado, and grape are all characterized as relatively salinity-sensitive crops, with avocado and grape tolerating NaCl concentrations only up to 50 mM and 15 mM, respectively (Ahmad & Anjum, 2020; Bernstein et al., 2004; Elhabashy, 2018; Mohammadkhani et al., 2016).

Salinity tolerance is a complex trait that involves the coordination of several interconnected mechanisms to minimize tissue damage upon salinity stress. Proposed mechanisms include minimizing salt ion entry into the plant, reducing salt ion loading into the xylem, maximizing salt ion compartmentalization in vacuoles, and retrieval of salt ion from the sap (Chen et al., 2018; Gupta & Huang, 2014; Munns et al., 2020; Tester & Davenport, 2003; Yang & Guo, 2018). Molecular mechanisms include the Salt Overly Sensitive (SOS) pathway at the plasma membrane, which regulates sodium ion ($Na^+$) efflux from the cytosol (Lin et al., 2009; Shi et al., 2000, 2003; Tester & Davenport, 2003; Yang et al., 2009; Zhu, 2002), and HKT1-type transporters, which contribute to reducing root to shoot $Na^+$ transport by retrieving $Na^+$ from the xylem (Davenport et al., 2007; Hauser & Horie, 2010; Møller et al., 2009; Rubio et al., 1995). Furthermore, intracellular compartmentalization of salt ions via vacuolar sequestration to reduce cytosolic toxicity is mediated by $H^+$/$Na^+$ antiporters, encoded by the *NHX1/2* genes (Bassil et al., 2019; Gonzalez et al., 2012; Guo et al., 2020; Gupta & Huang, 2014; Munns et al., 2016; Zhang & Blumwald, 2001). Such pathways are being explored to obtain salinity tolerance in different crop and non-crop species (Escalante-Pérez et al., 2009; Henderson et al., 2018; Shohan et al., 2019; Yang et al., 2009; Zhang et al., 2019).

Plants can additionally minimize salt entry via cellular barrier-mediated blockage of apoplastic transport. Apoplastic barriers can prevent bypass flow, which would otherwise allow $Na^+$ to enter the shoot through the transpiration stream (Chen et al., 2018; Wang et al., 2020). The root endodermis and exodermis are two cell barrier layers with highly specialized functions attributed to two notable features of their cell walls: (a) the Casparian strip and (b) the suberin lamella (Barberon et al., 2016; Doblas et al., 2017; Drapek et al., 2018; Enstone et al., 2003; Krishnamurthy et al., 2011; Wang et al., 2020). The Casparian strip, a paracellular deposition of lignin in the cell walls of the endodermis and exodermis, forces all apoplastic transport into the tightly regulated symplastic system (Lee et al., 2013; Naseer et al., 2012). In addition, suberin lamellae, composed mainly of long-chain fatty acids, impregnate the entire exodermis/endodermis cell wall, forming a hydrophobic barrier which helps regulate ion and water uptake (Enstone et al., 2003; Krishnamurthy et al., 2011; Serra et al., 2009).

Salinity influences both the timing and extent of suberization in apoplastic barriers, which in turn can affect the entrance of salt into vascular tissue (Byrt et al., 2018; Chen et al., 2011; Enstone et al., 2003; Wang et al., 2020). Apoplastic barrier-based control of $Na^+$ uptake occurs both in monocot and eudicot plants (Wang et al., 2020; Yeo et al., 1999). However, to date, there have been very few investigations regarding the development of apoplastic barriers in woody fruit and nut crop species. In addition, there are limited studies in woody perennial species investigating salinity stress responses at the cellular level using anatomical analysis based on imaging methodologies. In olive plants, suberization is thought to increase in response to drought stress, which in turn reduces root hydrodynamics (Tataranni et al., 2015). However, the precise effect of suberization on salt ion uptake is unknown. Evidence is emerging in citrus that suberin deposition may increase in response to salt stress in higher order roots, while higher suberin deposition in the exodermis combined with vacuolar $Na^+$ sequestration is associated with lower $Na^+$ content in leaves (Gonzalez et al., 2012; Rewald et al., 2012; Ruiz et al., 2016; Storey & Walker, 1998). In *Pistacia* species, the contribution of apoplastic barriers to salinity tolerance has hitherto not been examined.

Physiological studies on the effects of salinity on pistachio rootstocks have proposed multiple mechanisms which can contribute to salinity tolerance. Picchioni et al. showed that under salinity treatment, more $Na^+$ is sequestered in roots than stems (Picchioni et al., 1990). It has been hypothesized that increased proline levels provide osmoprotection in both leaves and roots for several pistachio rootstocks, including UCB1, a hybrid of *Pistacia atlantica* and *P. integerrima* (Akbari et al., 2018; Jamshidi Goharrizi et al., 2020; Rahneshan et al., 2018). Both *P. integerrima* (also known as PGI) and the hybrid UCB1 are popular commercial rootstocks with *P. vera* scion cultivars (Holtz et al., 2005; Zohary & Spiegl-Roy, 1975). Phenotypic studies assessed by leaf injury and shoot growth of the budded scion showed higher tolerance of UCB1 compared to *P. integerrima* under combined salinity and boron stresses (Ferguson et al., 2002). In an unbudded comparison of potential rootstock lines, UCB1 performs better in root sodium sequestration compared to several *P. vera* cultivars (Akbari et al., 2018). UCB1 can exclude up to 85%–90% of $Na^+$ from budded *P. vera* Kerman cv. shoots (Godfrey et al., 2019). Furthermore, UCB1 has lower sap $Na^+$ concentrations and lower wood $Na^+$ concentrations in the distal stem compared to *P. integerrima*, which suggests more efficient $Na^+$ exclusion from the shoots of UCB1 (Godfrey et al., 2019). Cumulatively, pistachio salinity tolerance appears to be a combination of multiple mechanisms working in tandem, with a prominent role for salt ion exclusion from the shoots. However, the exact mechanisms for salt exclusion remain unknown, especially at the cellular level.

Screens and studies of salinity tolerance in pistachio remain challenging. This is partially due to the high degree of genetic variability

that exists in each genotype, given that pistachio is both dioecious and wind-pollinated (Ahmad et al., 2003). Pistachio is a woody perennial species, which requires longer time to reach maturity and significantly greater investment for field trials than herbaceous annual crops. Therefore, there exist a pressing need to develop screening methods for young seedlings to quantitatively and qualitatively assess their relative performance under salinity stress.

Among the few studies that focus on salt tolerance in the rootstocks of woody perennial nut species, there is very limited information on fine roots, which is the main region for water and ion uptake, or on the root tips, where ions may accumulate (McCully, 1995, 1999; Ranathunge et al., 2011; Shao et al., 2021). Currently, there exists no detailed description of the root anatomy in pistachio rootstocks. To advance efforts in developing procedures for salinity tolerance screening, we used young seedlings in our study. We developed a fluorescence microscopy-based pipeline to investigate the localization of sodium and the differentiation of root endodermis and exodermis in salt-treated pistachio rootstocks across a developmental gradient characterized by xylem differentiation. Our results indicate that a combination of sodium sequestration and apoplastic barrier differentiation is involved in pistachio rootstocks' response to salinity stress, and that these responses are coordinated across a root maturation gradient.

## 2 | MATERIALS and METHODS

### 2.1 | Plant material and growing conditions

*P. integerrima* and UCB1 seeds were provided by the Foundation Plant Services, University of California, the Kresha Agricultural Nursery, and the Wolfskill Experimental Orchard.

Pistachio seeds were separated from shells and sterilized in a mixture of 5% (V/V) bleach and 1% (V/V) Tween-20 in deionized water. Seeds were germinated in vitro on ½ Murashige-Skoog (MS) medium at an adjusted pH of 5.7, containing 1% (W/V) sucrose, 0.1% (W/V) activated charcoal, and 0.75% (W/V) agarose. The media were supplemented with 4.5 μM 6-Benzylaminopurine, 0.5 μM indole-3-butyric acid, and 0.29 μM gibberellic acid (gibberellin $A_3$). Germinated seedlings were grown for 8 weeks for UCB1 and 10 weeks for *P. integerrima* in the same medium, at 22 ± 2°C using fluorescent light (100–150 mmol quanta PAR $m^{-2}$ $s^{-1}$) under long day conditions (16:8 hr light:dark). Plants were transferred to charcoal-free supplemented ½ MS medium for a minimum of 1 week prior to the start of the experiment.

### 2.2 | Salinity treatment

Seedlings were transferred to a fresh charcoal-free supplemented ½ MS medium for no-salt controls or the same medium containing 100 mM NaCl. The plants were grown for 1 week, under the conditions described above, before sectioning and further processing. Plant images were collected at the start and the end of the treatment for phenotypic assessment. Salt-treated plants were manually categorized into three groups based on their leaf phenotypes: (a) "high tolerance" when their leaf phenotype was indistinguishable from no-salt control plants, (b) "low tolerance" when over 75% of leaves showed burns and/or senescence, and (c) "moderate tolerance" when plants had an intermediate phenotype between that of "high tolerance" and "low tolerance".

### 2.3 | Sample collection

During sample collection, seedlings were imaged, removed from medium, and the roots carefully rinsed to remove residual media. Excess water was removed by careful dabbing with Kimwipes (Thermo Fisher, 34120), and the length and weight were measured for both the roots and the shoots. We assessed growth by fresh weight instead of dried weight due to the light weight of individual dried seedlings.

### 2.4 | Root phenotype quantification

Roots of harvested plants were gently spread out against a dissection mat and photographed with a ruler. ImageJ (https://imagej.nih.gov/ij/) was used to quantify the root length using the photographed ruler as the scale and using the segmented line tool to trace the root length. Root numbers were quantified using the multi-point tool in ImageJ, by assigning a point to each lateral root and reporting the final point count.

### 2.5 | Salt ion analysis

Roots from salt-treated and no-salt control seedlings were carefully washed twice with deionized water and then dried for 24 hr at 70°C. Three to five plants were pooled for roots and leaves samples to meet the minimum weight requirement for ion analysis. Samples were weighed and sealed in envelopes and stored with desiccant to avoid hydration prior to ion analysis. Ion analysis was performed using inductively coupled plasma-mass spectrometry at the Baxter Laboratory Ionomics Facility at the Donald Danforth Plant Science Center (https://www.baxterlab.org) according to established procedures (Ramirez-Flores et al., 2017).

### 2.6 | Fluorescence staining and microscopy

Root tips from all leaf phenotype groups were cut into 0.5 cm segments starting from the distal tip. Root tip segments were embedded in 5% (W/V) agarose (Sigma-Aldrich A9539) in deionized water and sectioned to 100 μm thickness using a vibratome (Vibratome 1000 Plus Sectioning System) as previously described (Pradhan

Mitra & Loqué, 2014). Sections were transferred into CoroNa Green incubation buffer (20 mM 3-(N-morpholino)propanesulfonic acid, 0.5 mM calcium sulfate, and 200 mM sorbitol). For CoroNa Green staining, 50 μg of CoroNa Green reagent (Thermo Fisher, C36676) was resuspended in 100 μl dimethyl sulfoxide, and this stock solution was further diluted in incubation buffer to prepare the 0.1 mM staining solution. Sections of both salt-treated plant roots and no-salt control roots were either incubated in staining solution or in incubation buffer as unstained controls for autofluorescence, for 16 hr in the dark at room temperature prior to imaging. SNARF-1 staining (Thermo Fisher, C1270) was performed using a protocol adapted from Rosquete et al. (Rosquete et al., 2019). Briefly, 1 μl of 10 mM SNARF-1 was diluted in 1 ml of CoroNa Green incubation buffer, and sections were incubated in this SNARF-1 solution in the dark for 3 hr at room temperature before imaging (Rosquete et al., 2019). Suberin staining was performed using an adapted protocol from Naseer et al. (Naseer et al., 2012). Briefly, sections were incubated in 0.1 mg/ml Fluorol Yellow 088 (Santa Cruz Biotechnology CAS-81-37-8) in lactic acid for 1 hr at 70°C in the dark, rinsed in double deionized water, and imaged mounted in 50% glycerol. Fluorescein diacetate (FDA) staining (Sigma, #F7378) was performed using an adapted protocol from Jones et al. (Jones et al., 2016). Briefly, live root sections were incubated in 4 μg/ml of FDA in incubation buffer for 5 min in the dark and imaged within 30 min.

### 2.7 | Image acquisition and analysis

A Zeiss 700 laser scanning confocal microscope was used for all imaging. Fluorescence signals of CoroNa Green (excitation 488 nm, 5% power, 493–800 nm emission collection) and CoroNa Green and SNARF-1 co-stain (excitation 488 nm, 15% power with 493–550 nm emission collection, 555 nm, 20% power with 566 to 800 nm emission collection) were acquired with a 20x air objective in CoroNa Green incubation buffer. Fluorescence signals of suberin (excitation 488 nm, 5% power, 493–800 nm emission collection) were acquired with a 20x air objective with the sample mounted in 50% (V/V) glycerol in deionized water. Autofluorescence signals from unstained samples were collected using identical imaging settings as those used for stained samples for each developmental zone, genotype, and treatment.

Quantification was performed using ImageJ (Schneider et al., 2012). Briefly, the confocal microscopy images were separated into groups based on xylem development. The groups were established as follows: zone 0 represented the youngest (least mature) differentiated root region in which only protoxylem is present, zone 1 represented the region of intermediate development in which both protoxylem and metaxylem are present, zone 2 represented the most mature region, in which development of secondary xylem has initiated. For each CoroNa Green sample imaged, a maximum intensity projection was generated from a Z-stack using the Zen Black (Zeiss) software. This allowed verification of the vacuolar identity via its shape and export of the data as a single image. $Na^+$-positive vacuoles were counted using the default multi-point tool in ImageJ, by manually selecting each vacuole and recording the final tally. For Fluorol Yellow 088 signal quantification, lines were drawn through the cell layer of interest, perpendicular to the radial cell walls of exported maximum intensity projections, using the segmented line tool in ImageJ. The intensity values corresponding to the radial cell walls were used to obtain the average fluorescence for the entire endodermis and exodermis cell layers in each section. During all signal intensity analyses, the signal intensity values from the unstained sections were subtracted from the values of the stained sections to control for autofluorescence. Fluorescence images presented in the manuscript were generated using either Zen Black or Imaris 9.6 (Oxford Instruments). Final figures were assembled in Adobe Illustrator (Adobe.com) or Inkscape (Inkscape.org).

### 2.8 | Statistical analysis

Multi-factor analysis of variance (ANOVA) was performed using R x 64 version 4.0.3 (R Core Team, 2017) in Rstudio (RStudio, PBC), version 1.3.1093 with the basic ANOVA function, and also in Statistical Analysis System (SAS Institute Inc), version 9. Least square means (LS-means) analysis was performed using the emmeans package (version 1.5.3) and the multcomp package (version 1.4-15) in R and the Statistical Analysis System. Final graphs were generated using Microsoft Excel and edited in Adobe Illustrator and Inkscape.

## 3 | RESULTS

### 3.1 | Phenotypic characterization of leaf tissue revealed a higher percentage of salt-tolerant plants in UCB1 compared to *P. integerrima*

In order to better understand salt tolerance in pistachios and to evaluate the root level response, we first established experimental conditions in a laboratory setting. Due to difficulties in obtaining and germinating *P. atlantica* seeds, we chose to focus on *P. integerrima* and UCB1 seedlings. We began by assessing the phenotypic response of UCB1 and *P. integerrima* seedlings under salt stress. UCB1 is known for its more robust growth, potentially due to hybrid vigor. As a result, *P. integerrima* of the same age as UCB1 is significantly smaller. Hence, in order to account for size effects on salinity tolerance and normalize for differences in biomass and salt ion content per gram tissue, we used size matching 8-week-old UCB1 plants and 10-week-old *P. integerrima* plants for all our assays. Individual plants were treated with 100 mM NaCl for 7 days and compared to 0 mM NaCl control plants of identical age (Figure 1a). Salt tolerance was qualitatively assessed by the severity of leaf senescence or burn symptoms and classified into “high tolerance”, “moderate tolerance”, and “low tolerance” as described earlier. Based on this phenotypic characterization, over 40% of UCB1 plants demonstrated high salinity tolerance, which is approximately twice the rate observed for *P.*


**FIGURE 1** More UCB1 seedlings exhibit high tolerance phenotype compared to *P. integerrima* under short-term salt treatment. (a) Representative high and low salinity tolerance phenotypes for the paternal genotype *P. integerrima* and hybrid line UCB1 after 1 week of 100 mM NaCl treatment. Pictures have not been corrected for perspective distortions. (b) Percentage of individuals in each genotype showing high, moderate, or low tolerance phenotypes. $n = 15$ for *P. integerrima*, 22 for UCB1

**FIGURE 2** Growth of *P. integerrima* and UCB1 under short-term salt treatment. (a) Quantification of fresh weight after 1-week salt treatment (NS, two-way ANOVA, $n = 7$–9 plants/treatment/genotype. Error bars = SEM). (b) Quantification of lateral roots (LRs) per plant (letters assigned by LS-means, $p = .05$, $n = 16$–17 plants/treatment/genotype. Error bars = SEM)

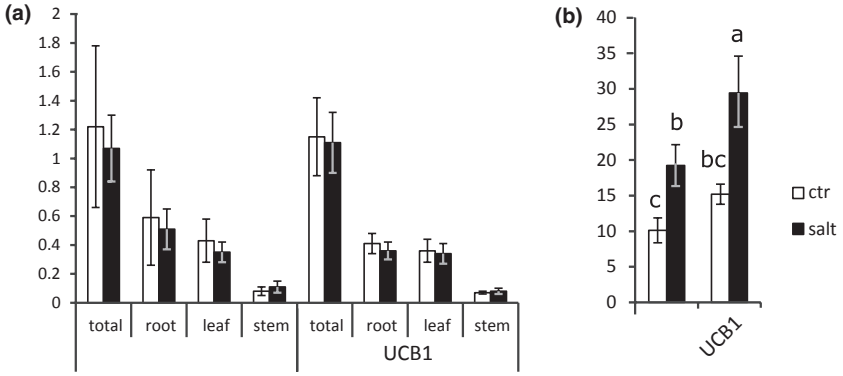


*integerrima* (Figure 1b). The higher percentage of UCB1 plants exhibiting the high tolerance leaf phenotype suggests an underlying difference between the two rootstocks, corroborating earlier studies (Ferguson et al., 2002; Godfrey et al., 2019).

We next examined the roots and shoots of salt-treated plants for developmental changes under short-term treatment. At the ages selected, the two genotypes had a virtually identical fresh weight (Figure 2a, NS, two-way ANOVA). After 1 week of salt treatment, neither *P. integerrima* nor UCB1 showed significant decreases in root or shoot growth (Figure 2a, NS, two-way ANOVA).

Root system architecture remodeling is known to occur as a result of salinity stress (Julkowska et al., 2014); thus, we assessed the root architecture of the treated plants. Although their root weights were comparable (Figure 2a), the UCB1 plants had more lateral roots compared to *P. integerrima*. Both genotypes showed an increased number of lateral roots after salt treatment, with a greater increase in UCB1 (Figure 2b, $p < .05$ between genotypes, $p < .01$ between treatment, two-way ANOVA, LS-means $p = .05$, Table S1, Figure S1). No significant difference in total lateral root length was observed between genotypes (Figure S2b, NS, two-way ANOVA). Based on these results, we concluded that a 1-week salinity stress treatment was sufficient to induce foliar phenotypes in laboratory settings, but insufficient to cause biomass changes. We reasoned that such an experimental setup enables the dissection of relatively early salinity responses without the compromising effect of an altered physiological status. This allows us to explore the initiation of salinity stress responses.

## 3.2 | Vacuolar $Na^+$ sequestration in UCB1

In order to investigate the mechanisms of salt tolerance, we visualized the cellular localization of $Na^+$ in live root sections with CoroNa Green, an indicator that exhibits increased green fluorescence emission upon $Na^+$ binding (Gonzalez et al., 2012; Park et al., 2009; Shao et al., 2021). Since abiotic stress induces root differentiation closer to the apical meristem (Cajero-Sanchez et al., 2019; Rost, 2011), we assessed the relationship between root tissue maturity and salinity

response. We investigated $Na^+$ localization across a root developmental gradient, characterized by the type and extent of xylem formation in the root tips (Figure 3a,b, Figure S3), with zone 0 as the youngest region and zone 2 as the oldest (Figure 3b, Figure S3).

We observed sodium signal in cortical parenchyma cell vacuoles of salt-treated UCB1 seedlings (Figure 3a). Cell viability was confirmed in the root cross sections via fluorescein diacetate staining, which measures both enzymatic activity (required to activate its fluorescence) and cell-membrane integrity (required for intracellular retention of their fluorescent product) (Figure S4). Comparison of all developmental zone vacuolar staining showed a notable increase in $Na^+$-positive vacuoles in salt-treated UCB1 compared to controls. This increase was not observed in *P. integerrima* (Figure 3c). The number of $Na^+$-positive vacuoles in UCB1 salt-treated plants was significantly increased compared to both *P. integerrima*-treated and control plants (Figure 3c), using least square means (LS-means) analysis with a threshold of $p = .05$. Two-way ANOVA did not identify any interaction between genotypes and treatments (Table S1).

The number of $Na^+$-positive vacuoles appeared to vary with the stages of xylem development. Thus, we analyzed them by each developmental zone (Figure 3b). The highest number of $Na^+$-stained vacuoles was observed in zone 1 of the UCB1 salt-treated plants (Figure 3d, LS-means $p = .05$), while *P. integerrima* showed minimal $Na^+$-positive vacuoles regardless of treatment, with no significant zone-specific difference (Figure 3a,c,d).

Co-localization with the established red fluorescent vacuolar marker SNARF-1 (Rosquete et al., 2019) demonstrated that CoroNa Green indeed exhibited vacuolar localization (Figure 4a–c). The dyes under our imaging conditions did not exhibit spectral crosstalk. CoroNa Green-labeled sections, without SNARF-1, displayed vacuolar signal only in the CoroNa Green channel (Figure 4d), and not in the SNARF-1 channel (Figure 4e,f). Sections stained with only SNARF-1, without CoroNa Green, showed signal only in the SNARF-1 channel (Figure 4h) and not in the CoroNa Green channel (Figure 4g,i). Furthermore, neither CoroNa Green nor SNARF-1 signals in the vacuole are compromised by plant tissue autofluorescence (Figure S5). The verification of the signal specificity confirms that the observed vacuolar $Na^+$ localization in Figure 4a–c is authentic. Cumulatively, our data clearly demonstrated increased sodium sequestration in the vacuoles of UCB1 roots compared to *P. integerrima*.

Since the vacuolar localization of $Na^+$ suggests sequestration in root tissue, we measured the $Na^+$ concentration in the roots of *P. integerrima* and UCB1 after 1 week of salt treatment. Both UCB1 and *P. integerrima* roots showed a significant $Na^+$ increase (Figure S6, two-way ANOVA, $p < .01$ between treatment, Table S1), though the increase in UCB1 plants was slightly less than that observed in *P. integerrima* (Figure S6).

In leaf tissue, the changes in ion concentration were more pronounced. A significant increase of $Na^+$ ions in the leaves of salt-treated plants was observed (Figure S6, two-way ANOVA, $p < .01$

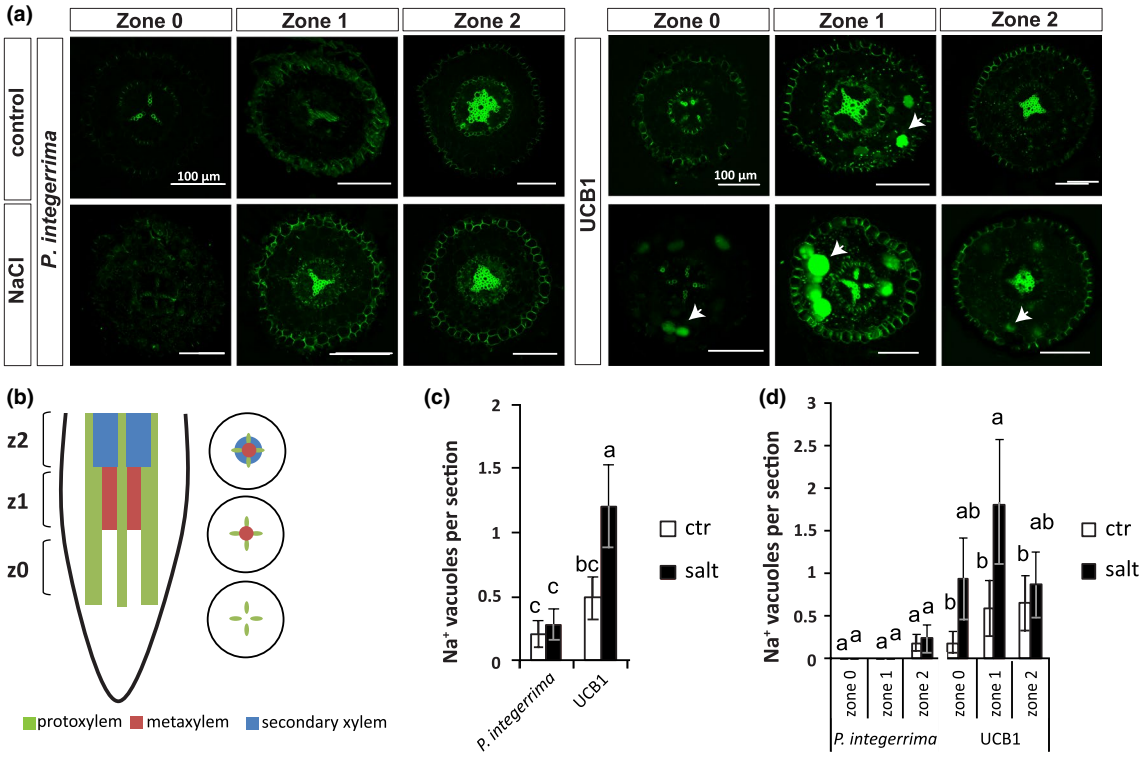


**FIGURE 3** Increased vacuolar sodium sequestration in UCB1 compared to *P. integerrima*. (a) *P. integerrima* and UCB1 root tip sections stained for $Na^+$, vacuoles indicated by arrowheads. 3D construction is shown for zone 1 salt-treated UCB1. (b) Diagram of root tip zones as staged by xylem development. z0 = zone 0, z1 = zone 1, z2 = zone 2. (c) Quantification of average number of vacuoles per cross section. (d) Quantification of average number of $Na^+$ vacuoles staged by xylem development (Letters assigned by LS-means, $p = .05$. $n = 15–51$ sections/zone/genotype from 3–5 plants. Error bars = SEM)

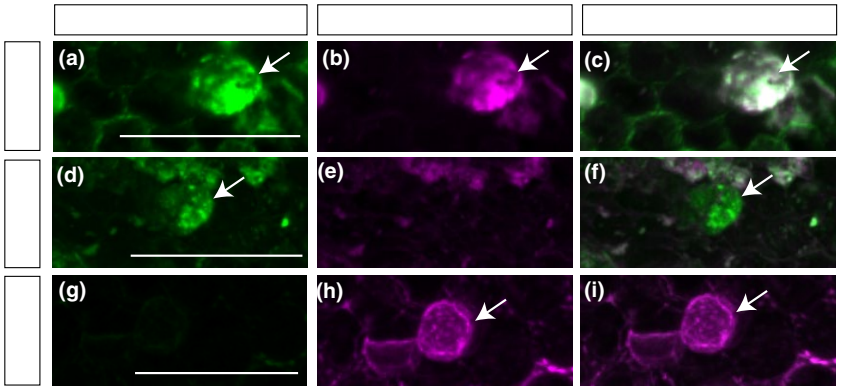


**FIGURE 4** Sodium staining in UCB1 co-localizes with a vacuolar marker. (a–c) Co-staining of $Na^+$ with CoroNa green (a) and SNARF-1 for the vacuole (b) showed co-localization in the vacuoles of salt-treated UCB1 root cross section (c). Vacuoles are indicated by arrows. (d–f) CoroNa Green staining alone displayed signal in the CoroNa Green channel (d), and not in the SNARF-1 channel (e and f). (g–i) Sections stained with only SNARF-1, without CoroNa Green, show no signal in the CoroNa Green channel (g and i)

between treatments, Table S1). In addition, salt-treated UCB1 plants showed lower $Na^+$ concentrations than *P. integerrima* (Figure S6, LS-means $p = .05$). Our leaf data are consistent with earlier studies, demonstrating that UCB1 has lower $Na^+$ concentrations in leaf tissues compared to *P. integerrima* under salt treatment (Ferguson et al., 2002).

We also measured the $K^+$ concentration in roots and leaves, given that its accumulation during salt stress is associated with increased salinity tolerance (Shabala et al., 2005; Volkov et al., 2004). We did not observe significant changes in root $K^+$ concentrations of either UCB1 or *P. integerrima* under salt treatment, though there was consistently higher $K^+$ concentration in UCB1 roots compared to *P. integerrima* ($p < .01$ between genotype, two-way ANOVA. LS-means $p = .05$, Figure S6, Table S1). Interestingly, in the leaf tissues, there was no difference between *P. integerrima* and UCB1 no-salt controls, while the salt treatment appeared to lower the leaf $K^+$ content in UCB1 more than that of *P. integerrima* (Figure S6, two-way ANOVA, $p < .05$ between treatment, LS-means $p = .05$).

### 3.3 | Increased suberin deposition at the endodermis and exodermis of UCB1

We observed a slight increase of CoroNa Green signal in the cell walls of the endodermis and the exodermis of salt-treated plants during imaging (Figure 3a). The origin of the signal is attributable to the stain and not to autofluorescence (Figure S5). Therefore, we investigated whether the development of suberin lamellae in these two cell layers is regulated as part of the salinity stress response. We used a well-established methodology for suberin detection via staining with the lipophilic fluorochrome, Fluorol Yellow 088 (Kreszies et al., 2019; Lux et al., 2005), to quantify suberin accumulation.

First, we analyzed the effect of salinity on suberin deposition for each genotype across a root developmental gradient. Higher suberin deposition was observed throughout the apoplastic barriers of UCB1 compared to *P. integerrima*, a pattern that was maintained or accentuated under salt treatment (Figure 5a). After correcting for autofluorescence in each developmental zone, genotype, and treatment, our quantification demonstrated statistically significant change in suberization under salt treatment. UCB1 showed an increase in endodermis suberization in zone 0 under salt treatment (Figure 5d, Table S1. $p < .01$ between treatment, two-way ANOVA. $p = .05$, LS-means). This corresponds to the youngest region of the root tip with the high developmental plasticity. Furthermore, when all developmental zones are considered together, a significant increase was observed between the endodermis of UCB1 compared to *P. integerrima* under salt treatment (Figure 5b, Table S1. $p < .01$ between genotype, treatment, and tissue, three-way ANOVA. $p = .05$, LS-means). In contrast to the endodermis, the exodermis of *P. integerrima* had a zone-specific increase of suberization in zone 1 compared to zone 0 of salt-treated plants (Figure 5c, Table S1. $p < .05$, two-way ANOVA. $p = .05$, LS-means).

It is worth noting that three-way ANOVA analysis across all zones (Figure 5b) indicates that the difference in suberin deposition between endodermis and exodermis is genotype dependent (Table S1, $p < .05$, genotype by tissue interaction, three-way ANOVA) and that endodermis and exodermis respond to salinity stress differently as shown by the aforementioned analysis (Table S1, $p < .05$, treatment by tissue interaction, three-way ANOVA).

## 4 | DISCUSSION

In light of climate change-based drought conditions which have led to increased soil salinity, pistachio, a crop with relative high salinity and drought tolerance, is poised to become an important model to investigate the mechanisms of abiotic stress response (Ahmad & Prasad, 2012; Bailey-Serres et al., 2019; Jazi et al., 2016). Studies of salt stress and salinity tolerance in pistachios so far have focused on whole-plant physiological responses (Ferguson et al., 2002; Godfrey et al., 2019; Karimi et al., 2009; Picchioni et al., 1990). While salinity stress has been extensively studied in diverse species, there is

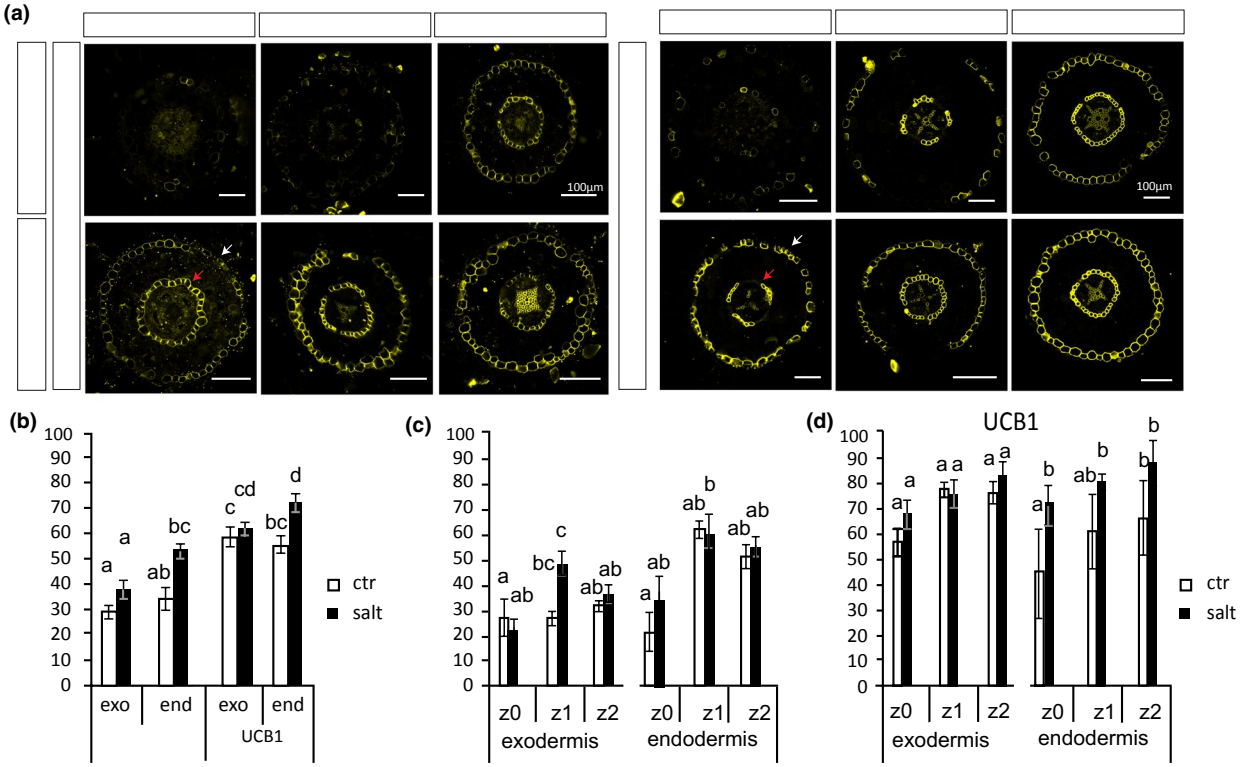


**FIGURE 5** Suberin deposition is enhanced in apoplastic barriers under salinity stress. (a) Cross sections of root tips in both *P. integerrima* and UCB1, stained with Fluorol Yellow 088, showed increased suberization at the exodermis (white arrow) and endodermis (red arrow). (b) Quantification of suberin fluorescence intensity (a. u.) in exodermis and endodermis across all cross sections under control and salt (100 mM NaCl) treatment. (c and d) Analysis of suberin fluorescence in zones staged by xylem development between control and 100 mM salt treatment in (c) *P. integerrima* and (d) UCB1 (Letters assigned by LS means, $p = .05$. $n = 28–62$ sections/3-5 plants for b. $n = 3–28$ sections/zone/genotype/treatment for c and d. Error bars = SEM)

limited information on the root of woody nut trees, such as pistachio. This report represents a foundational study of the root responses to salinity stress, from the physiological to the cellular level, which can be built upon and expanded to include different species to obtain a more comprehensive view of salinity tolerance.

## 4.1 | Short-term salinity treatment as an experimental approach to detect salinity responses in pistachio

One-week salinity treatment was sufficient to induce variation in leaf damage between UCB1 and *P. integerrima*, and between individuals of the same genotype. Even with intraspecific variations, the higher percentage of UCB1 individuals with no foliar damage suggests that UCB1 is more tolerant than *P. integerrima*. This corroborates earlier field studies, in which salinity and boron caused less damage in leaves of scions grafted to UCB1 compared to those grafted to *P. integerrima* (Ferguson et al., 2002). The selection of a 1-week, short-term treatment for analysis likely reveals early response mechanisms to salinity stress, since no major effects in overall plant growth and biomass have occurred yet.

Notably, there is a slight increase in the number of lateral roots under salinity treatment. In Arabidopsis, under moderate salinity stress, the number of lateral root emergence can increase, while lateral root length decreases as part of root remodeling. However, this increase disappears under high salinity tolerance (Julkowska et al., 2014, 2017; Zolla et al., 2010). Zolla et al. hypothesized that this behavior is part of a stress-induced morphogenic response (SIMR), similar to that observed under ultraviolet light, heavy metal, and mechanical stress. The abiotic stresses remove the developmental arrests of lateral root primordia, potentially via the auxin signaling pathway (Zolla et al., 2010). Thus, the increase in lateral root emergences we observed in pistachio may be attributable to salinity-induced SIMR.

## 4.2 | UCB1 vacuolar sodium sequestration

UCB1 plants showed a higher vacuolar $Na^+$ sequestration capacity compared to *P. integerrima* (Figure 3), which may be a result of increased vacuolar $Na^+$ import and/or a result of increased vacuolar $Na^+$ retention. Overexpression of *NHX1*, a salt ion antiporter, increases salt tolerance in diverse species such as wheat, rice, tomato, and mung bean (Kumar et al., 2017; Moghaieb et al., 2014; Zeng et al., 2018;

Zhang & Blumwald, 2001). UCB1 may exhibit higher salinity tolerance compared to *P. integerrima* due to an increased efficiency at vacuolar sequestration via increased expression or activity of salt ion antiporters such as the *NHX1* (Bassil et al., 2019; Guo et al., 2020; Gupta & Huang, 2014). Retention of $Na^+$ in the vacuole can also be affected by the back-leak of $Na^+$ into the cytosol via cation channels or tonoplast permeability (Isayenkov et al., 2010; Leach et al., 1990; Munns et al., 2016, 2020). It remains unknown whether these also contribute to the increased efficiency of vacuolar sequestration in UCB1. Future analyses of expression and activity of salt ion antiporters, along with other $Na^+$-permeable cation channels, tonoplast lipid composition, and a abiotic stress response markers, could help dissect the main molecular pathways in UCB1 for salinity tolerance (Deinlein et al., 2014; Gupta & Huang, 2014; Yang et al., 2009; van Zelm et al., 2020).

The difference in leaf sodium concentration between genotypes suggests that transport of sodium to the leaves of UCB1 is more tightly regulated. Since numerous studies in various species have identified sequestration and apoplastic barrier differentiation in roots to be important for shoot salinity tolerance (Gonzalez et al., 2012; Guo et al., 2020; Krishnamurthy et al., 2011; Wang et al., 2020), this combination likely contributes to the observed salt distribution in UCB1 as well. The duo mechanisms of decreasing salt ion entry into the plant and then further sequestering it within the root can substantially decrease the amount of salt that reaches the shoot. This underscores the importance of investigating tissue and organ ion accumulation in conjunction with subcellular localization.

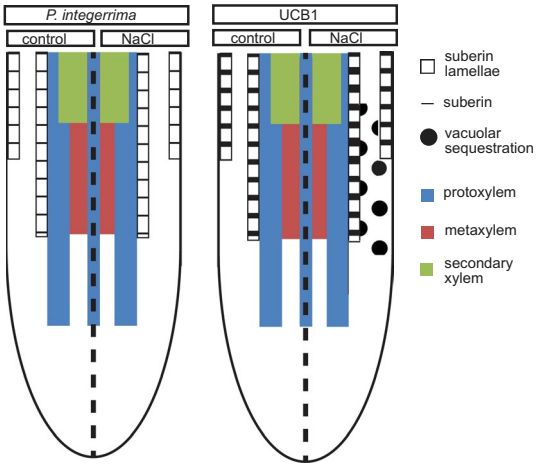


**FIGURE 6** Model of *P. integerrima* and UCB1 root tip response to short-term salt treatment. Under salinity stress, UCB1 plants, in contrast to *P. integerrima*, are able to sequester excess $Na^+$ in the vacuoles of cortical parenchyma cells in the root tips. Under control conditions, UCB1 deposits more suberin in cellular barriers. The deposition difference between the two genotypes is maintained under salinity stress

## 4.3 | Apoplastic barriers as a line of defense

A notable effect of salinity stress we observed was the increase in the suberin deposition of the endodermis (Figure 5). Higher baseline levels of suberization can reduce the exposure of root cells to toxic ion levels at early stages of salt stress and further minimize salt ion entry into the roots. This can reduce osmotic stress, ionic toxicity, and help preserve the health of the root cells as have been proposed in other species such as rice and citrus (Ruiz et al., 2016; Vishal et al., 2019).

Vacuolar sequestration and suberin deposition both require energy input (Tyerman et al., 2019). The increased basal level in suberin deposition at the endodermis of UCB1 indicates an early energy investment to enforce salt exclusion from the vascular cylinder. Selection pressure for crop varieties with increased apoplastic barrier suberization has been shown for barley (Kreszies et al., 2020), indicating that this trait is present in monocots. The popularity of UCB1 in pistachio breeding suggests that a similar selection may take place in woody perennial crops.

## 4.4 | Vacuolar sequestration and suberin deposition follow the root developmental gradient

Sodium uptake, transport, and sequestration are closely linked to root developmental stages. Thus, we proposed a model of sodium distribution based on the pistachio root developmental gradient (Figure 6). Sodium uptake and transport at the youngest zone, zone 0, are relatively unhindered by apoplastic barriers, and the uptake is accompanied by vacuolar sequestration to minimize the impact of salt ions. In zone 1, the second developmental zone, the peak of $Na^+$ sequestration in parenchyma cells likely reflects their higher vacuolar storage capacity and maturation status compared to the meristematic zone 0. This corroborates the pattern of vacuolar $Na^+$ sequestration observed in various species (Bojórquez-Quintal et al., 2014; Wu et al., 2015, 2019). It is also possible that more ionic uptake occurs in zone 1 due to the increase in the number of mature vessel elements compared to zone 0 (Baum et al., 2002; Wachsman et al., 2015), and the higher rate of water and ion flow could be reflected in the amount of sodium sequestered in the vacuoles. Entry of sodium to the third developmental zone, zone 2, may be more tightly controlled due to the extensive suberization of apoplastic barriers, resulting in enhanced blockage of apoplastic transport and absorption (Barberon, 2017; Krishnamurthy et al., 2011; Ranathunge et al., 2011; Serra et al., 2009; Wang et al., 2020). This could lead to a reduction in the rate of zone 2 ion entry and reduced vacuolar sequestration compared to the younger developmental zones.

Our observed vacuolar sequestration, specifically in cortical parenchyma cells, corroborates earlier work in citrus rootstocks (Gonzalez et al., 2012). Similar to citrus, not all cells in the root cortex showed significant vacuolar sequestration, and this behavioral variation within a single cell type indicates cellular heterogeneity in cell health and/or sequestration potential. The type of heterogeneity that exists in cell populations is currently receiving increased attention in various experimental systems such as cell behavior within seed populations (Bradford, 2018). Single cell studies will be required to assay the variation in sequestration potential at the cellular level,

such as cell-by-cell examination of *NHX* expression. The responses of other subcellular compartments, such as different endosomes/vesicles, and cell type specificity (Oh et al., 2015), are additional layers of complexity which can be considered in future studies.

The development of the apoplastic barriers is highly responsive to abiotic stress (Barberon, 2017; Byrt et al., 2018; Chen et al., 2018; Enstone et al., 2003; Kreszies et al., 2019; Wang et al., 2020) and contributes to salinity tolerance (Chen et al., 2018; Krishnamurthy et al., 2011; Wang et al., 2020). An analysis by developmental zones showed that the greatest increase in endodermis suberin deposition in UCB1, under salinity stress, occurred in the youngest zone (Figure 5d), which represents the region with the highest plasticity (Rost, 2011). Our results corroborate earlier findings in maize, barley, and rice indicating that development of the apoplastic barrier occurs closer to the root tip in response to salinity and other abiotic stresses (Kreszies et al., 2019; Shen et al., 2015; Vishal et al., 2019). It is possible that the difference in apoplastic barrier differentiation response during salt stress contributed to the difference in salinity tolerance between the observed pistachio genotypes.

Salinity stress induces overall modifications in the cell wall and its components, including suberin, lignin, and polysaccharide deposition (Byrt et al., 2018; Rui & Dinneny, 2020; Wang et al., 2020). Additional studies are needed to determine if the overall regulation of polysaccharide biosynthesis and deposition changes in pistachio to minimize salt ion entry and limit toxic ion transport to the leaves (Byrt et al., 2018). In addition, interaction between the root and the local microbiota has been shown to affect suberin deposition at the endodermis in Arabidopsis and to increase its salinity tolerance (Salas-González et al., 2020). It remains to be seen whether the microbiota significantly contributes to pistachio salinity tolerance by affecting its endodermal and exodermal suberin deposition.

## 5 | CONCLUSION

Based on our data and the existing literature, we propose a model describing aspects of sodium distribution in pistachio, with respect to root developmental gradients, under salinity stress. Our study, based on an initial anatomical characterization of pistachio roots under salinity stress, suggests that both root development and cell type specificity can contribute to salinity tolerance. During salinity stress, enhanced suberin deposition at the apoplastic barriers and vacuolar sequestration can contribute to $Na^+$ exclusion from the shoot. Notably, given that the peak of vacuolar sequestration and changes in suberization occur at the root tips, prior to the formation of the metaxylem, the response of the youngest developmental zones likely plays a critical role in the effectiveness of the salinity stress response. Together, the two mechanisms can contribute to a more efficient shoot $Na^+$ exclusion and prevent accumulation of toxic ion levels in the leaves.

Our foundational study can be referenced in future investigations of the cellular responses to salinity. The natural variation within woody perennial species, such as pistachio, can be exploited to identify and elucidate natural adaptation mechanisms of abiotic stress. With the anticipated availability of pistachio rootstock genomes, the aforementioned mechanisms may be understood at the molecular level in the not-so-distant future.

## ACKNOWLEDGMENTS

We thank P. J. Brown and M. R. Rosquete for their critical comments and suggestions. This study was supported by the Pistachio Board of CA HC-2017-22, HC-2019-21 awards, and the U.S. Department of Agriculture award CA-D-PLS-2132-H to G.D.

## CONFLICT OF INTEREST

The authors declare no conflict of interest associated with the work described in this manuscript.

## AUTHOR CONTRIBUTIONS

SZ, AQ, TW, LF, JJ, and GD conceived research. SZ, AQ, OKB, SM, ASH, GD, TW, and TL performed research. SZ, AQ, OKB, SM, ASH, YS, TC, JJ, TW, and GD analyzed data. SZ and GD wrote the manuscript. All the authors edited and accepted the final version of the manuscript.

## ORCID

*Shuxiao Zhang* https://orcid.org/0000-0002-0975-0962
*Alessandra Quartararo* https://orcid.org/0000-0001-7021-3464
*Oliver Karl Betz* https://orcid.org/0000-0001-9979-2391
*Angelo Schuabb Heringer* https://orcid.org/0000-0002-2723-7353
*Thu Le* https://orcid.org/0000-0001-8629-5396
*Yuhang Shao* https://orcid.org/0000-0002-6234-2802
*Louise Ferguson* https://orcid.org/0000-0002-9520-078X
*Judy Jernstedt* https://orcid.org/0000-0003-0575-0938
*Thomas Wilkop* https://orcid.org/0000-0001-9066-5513
*Georgia Drakakaki* https://orcid.org/0000-0002-3949-8657

## REFERENCES

Ahmad, P., & Prasad, M. (2012). Abiotic stress responses in plants. Abiotic Stress New Res. https://doi.org/10.1007/978-1-4614-0634-1

Ahmad, R., & Anjum, M. A. (2020). Physiological and molecular basis of salinity tolerance in fruit crops. In S. Anoop Kumar & H. Chengxiao (Eds.), *Fruit crops*. Elsevier. https://doi.org/10.1016/b978-0-12-818732-6.00032-0

Ahmad, R., Ferguson, L., & Southwick, S. M. (2003). Identification of Pistachio (Pistacia vera L.) Nuts with Microsatellite Markers. *Journal of the American Society for Horticultural Science*, *128*, 898–903. https://doi.org/10.21273/JASHS.128.6.0898

Akbari, M., Mahna, N., Ramesh, K., Bandehagh, A., & Mazzuca, S. (2018). Ion homeostasis, osmoregulation, and physiological changes in the roots and leaves of pistachio rootstocks in response to salinity. *Protoplasma*, *255*, 1349–1362. https://doi.org/10.1007/s00709-018-1235-z

Bailey-Serres, J., Parker, J. E., Ainsworth, E. A., Oldroyd, G. E. D., & Schroeder, J. I. (2019). Genetic strategies for improving crop yields. *Nature*, *575*, 109–118. https://doi.org/10.1038/s41586-019-1679-0

Barberon, M. (2017). The endodermis as a checkpoint for nutrients. *New Phytologist*, *213*, 1604–1610. https://doi.org/10.1111/nph.14140

Barberon, M., Vermeer, J. E. M., De Bellis, D., Wang, P., Naseer, S., Andersen, T. G., Humbel, B. M., Nawrath, C., Takano, J., Salt, D. E., & Geldner, N. (2016). Adaptation of root function by nutrient-induced plasticity of endodermal differentiation. *Cell*, *164*, 447–459. https://doi.org/10.1016/j.cell.2015.12.021

Bassil, E., Zhang, S., Gong, H., Tajima, H., & Blumwald, E. (2019). Cation specificity of vacuolar NHX-type cation/$H^+$ Antiporters 1[OPEN]. *Plant Physiology*, *179*, 616–629.

Baum, S. F., Dubrovsky, J. G., & Rost, T. L. (2002). Apical organization and maturation of the cortex and vascular cylinder in Arabidopsis thaliana (Brassicaceae) roots. *American Journal of Botany*, *89*, 908–920. https://doi.org/10.3732/ajb.89.6.908

Bernstein, N., Meiri, A., & Zilberstaine, M. (2004). Root growth of avocado is more sensitive to salinity than shoot growth. *Journal of the American Society for Horticultural Science*, *129*, 188–192. https://doi.org/10.21273/JASHS.129.2.0188

Bojórquez-Quintal, E., Velarde-Buendía, A., Ku-González, Á., Carillo-Pech, M., Ortega-Camacho, D., Echevarría-Machado, I., Pottosin, I., & Martínez-Estévez, M. (2014). Mechanisms of salt tolerance in habanero pepper plants (Capsicum chinense Jacq.): Proline accumulation, ions dynamics and sodium root-shoot partition and compartmentation. *Frontiers in Plant Science*, *5*, 1–14.

Bradford, K. J. (2018). Interpreting biological variation: Seeds, populations and sensitivity thresholds. *Seed Science Research*, *28*, 158–167. https://doi.org/10.1017/S0960258518000156

Byrt, C. S., Munns, R., Burton, R. A., Gilliham, M., & Wege, S. (2018). Root cell wall solutions for crop plants in saline soils. *Plant Science*, *269*, 47–55. https://doi.org/10.1016/j.plantsci.2017.12.012

Cajero-Sanchez, W., Aceves-Garcia, P., Fernández-Marcos, M., Gutiérrez, C., Rosas, U., García-Ponce, B., & Álvarez-Buylla, E. R. de la Sánchez, M. D. L. P., & Garay-Arroyo, A. (2019). Natural root cellular variation in responses to osmotic stress in arabidopsis thaliana accessions. *Genes (Basel)*, *10*, 1–23. https://doi.org/10.3390/genes10120983

Chen, M., Yang, Z., Liu, J., Zhu, T., Wei, X., Fan, H., & Wang, B. (2018). Adaptation mechanism of salt excluders under saline conditions and its applications. *International Journal of Molecular Sciences*, *19*(11), 3668. https://doi.org/10.3390/ijms19113668

Chen, T., Cai, X., Wu, X., Karahara, I., Schreiber, L., & Lin, J. (2011). Casparian strip development and its potential function in salt tolerance. *Plant Signaling & Behavior*, *6*, 1499–1502. https://doi.org/10.4161/psb.6.10.17054

Davenport, R. J., Muñoz-Mayor, A., Jha, D., Essah, P. A., Rus, A., & Tester, M. (2007). The $Na^+$ transporter AtHKT1;1 controls retrieval of $Na^+$ from the xylem in Arabidopsis. *Plant, Cell and Environment*, *30*, 497–507.

Deinlein, U., Sephan, A. B., Horie, T., Luo, W., Xu, G., & Schroeder, J. I. (2014). Plant salt-tolerance mechanisms. *Trends in Plant Science*, *19*, 371–379. https://doi.org/10.1016/j.tplants.2014.02.001

Doblas, V. G., Geldner, N., & Barberon, M. (2017). The endodermis, a tightly controlled barrier for nutrients. *Current Opinion in Plant Biology*, *39*, 136–143. https://doi.org/10.1016/j.pbi.2017.06.010

Drapek, C., Sparks, E. E., Marhavy, P., Taylor, I., Andersen, T. G., Hennacy, H. H., Gelder, N., & Benfey, P. N. (2018). Minimum requirements for changing and maintaining endodermis cell identity in the Arabidoopsis root. *Nature Plants*, *4*, 586–595.

El-habashy, S. (2018). In vitro Evaluation and Selection for Salinity Tolerance in Some Citrus Rootstock Seedlings. *Journal of Horticultural Science & Ornamental Plants*, *10*, 17–27. https://doi.org/10.5829/idosi.jhsop.2018.17.27

Enstone, D. E., Peterson, C. A., & Ma, F. (2003). Root Endodermis and Exodermis: Structure, Function, and Responses to the Environment. *Journal of Plant Growth Regulation*, 335–351. https://doi.org/10.1007/s00344-003-0002-2

Escalante-Pérez, M., Lautner, S., Nehls, U., Selle, A., Teuber, M., Schnitzler, J. P., Teichmann, T., Fayyaz, P., Hartung, W., Polle, A., & Fromm, J. (2009). Salt stress affects xylem differentiation of grey poplar (Populus x canescens). *Planta*, *229*, 299–309.

Ferguson, L., Poss, J. A., Grattan, S. R., Grieve, C. M., Wang, D., Wilson, C., Donovan, T. J., & Chao, C.-T. (2002). Pistachio rootstocks influence scion growth and ion relations under salinity and boron stress. *Journal of the American Society for Horticultural Science*, *127*, 194–199. https://doi.org/10.21273/JASHS.127.2.194

Godfrey, J. M., Ferguson, L., Sanden, B., Tixier, A., Sperling, O., Grattan, S. R., & Zwieniecki, M. A. (2019). Sodium interception by xylem parenchyma and chloride recirculation in phloem may augment exclusion in the salt tolerant Pistacia genus: Context for salinity studies on tree crops. *Tree Physiology*, 1–15. https://doi.org/10.1093/treephys/tpz054

Gonzalez, P., Syvertsen, J. P., & Etxeberria, E. (2012). Sodium distribution in salt-stressed citrus rootstock seedlings. *HortScience*, *47*, 1504–1511. https://doi.org/10.21273/HORTSCI.47.10.1504

Guo, Q., Tian, X. X., Mao, P. C., & Meng, L. (2020). Overexpression of Iris lactea tonoplast $Na^+/H^+$ antiporter gene IlNHX confers improved salt tolerance in tobacco. *Biologia Plantarum*, *64*, 50–57.

Gupta, B., & Huang, B. (2014). Mechanism of salinity tolerance in plants: Physiological, biochemical, and molecular characterization *International Journal of Genomics*, *2014*, 1–18. https://doi.org/10.1155/2014/701596

Hauser, F., & Horie, T. (2010). A conserved primary salt tolerance mechanism mediated by HKT transporters: A mechanism for sodium exclusion and maintenance of high $K^+/Na^+$ ratio in leaves during salinity stress. *Plant, Cell and Environment*, *33*, 552–565.

Henderson, S. W., Dunlevy, J. D., Wu, Y., Blackmore, D. H., Walker, R. R., Edwards, E. J., Gilliham, M., & Walker, A. R. (2018). Functional differences in transport properties of natural HKT1;1 variants influence shoot $Na^+$ exclusion in grapevine rootstocks. *New Phytologist*, *217*, 1113–1127.

Holtz, B., Ferguson, L., Parfitt, D., Allen, G., & Radoicich, R. (2005). Rootstock production and budding. Pist Prod Man, 74–79.

Isayenkov, S., Isner, J. C., & Maathuis, F. J. M. (2010). Vacuolar ion channels: Roles in plant nutrition and signalling. *FEBS Letters*, *584*, 1982–1988. https://doi.org/10.1016/j.febslet.2010.02.050

Jamshidi Goharrizi, K., Amirmahani, F., & Salehi, F. (2020). Assessment of changes in physiological and biochemical traits in four pistachio rootstocks under drought, salinity and drought + salinity stresses. *Physiologia Plantarum*, *168*, 973–989.

Jazi, M. M., Khorzoghi, E. G., Botanga, C., & Seyedi, S. M. (2016). Identification of reference genes for quantitative gene expression studies in a non-model tree pistachio (Pistacia vera L.). *PLoS One*, *11*, 1–16.

Jones, K., Kim, D. W., Park, J. S., & Khang, C. H. (2016). Live-cell fluorescence imaging to investigate the dynamics of plant cell death during infection by the rice blast fungus Magnaporthe oryzae. *BMC Plant Biology*, *16*, 1–8. https://doi.org/10.1186/s12870-016-0756-x

Julkowska, M. M., Hoefsloot, H. C. J., Mol, S., Feron, R., De Boer, G. J., Haring, M. A., & Testerink, C. (2014). Capturing arabidopsis root architecture dynamics with root-fit reveals diversity in responses to salinity. *Plant Physiology*, *166*, 1387–1402. https://doi.org/10.1104/pp.114.248963

Julkowska, M. M., Koevoets, I. T., Mol, S., Hoefsloot, H., Feron, R., Tester, M. A., Keurentjes, J. J. B., Korte, A., Haring, M. A., de Boer, G.-J., & Testerink, C. (2017). Genetic components of root architecture remodeling in response to salt stress. *The Plant Cell*, *29*, 3198–3213. https://doi.org/10.1105/tpc.16.00680

Karimi, S., Rahemi, M., Maftoun, M., & Eshghi, T. V. (2009). Effects of long-term salinity on growth and performance of two pistachio (Pistacia L.) rootstocks. *Australian Journal of Basic and Applied Sciences*, *3*, 1630–1639.

Kreszies, T., Eggels, S., Kreszies, V., Osthoff, A., Shellakkutti, N., Baldauf, J. A., Zeisler-Diehl, V. V., Hochholdinger, F., Ranathunge, K., &

Schreiber, L. (2020). Seminal roots of wild and cultivated barley differentially respond to osmotic stress in gene expression, suberization, and hydraulic conductivity. *Plant, Cell and Environment*, *43*, 344–357. https://doi.org/10.1111/pce.13675

Kreszies, T., Shellakkutti, N., Osthoff, A., Yu, P., Baldauf, J. A., Zeisler-Diehl, V. V., Ranathunge, K., Hochholdinger, F., & Schreiber, L. (2019). Osmotic stress enhances suberization of apoplastic barriers in barley seminal roots: Analysis of chemical, transcriptomic and physiological responses. *New Phytologist*, *221*, 180–194. https://doi.org/10.1111/nph.15351

Krishnamurthy, P., Ranathunge, K., Nayak, S., Schreiber, L., & Mathew, M. K. (2011). Root apoplastic barriers block $Na^+$ transport to shoots in rice (Oryza sativa L.). *Journal of Experimental Botany*, *62*, 4215–4228. https://doi.org/10.1093/jxb/err135

Kumar, S., Kalita, A., Srivastava, R., & Sahoo, L. (2017). Co-expression of arabidopsis NHX1 and bar improves the tolerance to salinity, oxidative stress, and herbicide in transgenic mungbean. *Frontiers in Plant Science*, *8*, 1–18. https://doi.org/10.3389/fpls.2017.01896

Leach, R. P., Wheeler, K. P., Flowers, T. J., & Yeo, A. R. (1990). Molecular markers for ion compartmentation in cells of higher plants: II. Lipid composition of the tonoplast of the halophyte suaeda maritima (L.) Dum. *Journal of Experimental Botany*, *41*, 1089–1994. https://doi.org/10.1093/jxb/41.9.1089

Lee, Y., Rubio, M. C., Alassimone, J., & Geldner, N. (2013). A mechanism for localized lignin deposition in the endodermis. *Cell*, *153*, 402–412. https://doi.org/10.1016/j.cell.2013.02.045

Lin, H., Yang, Y., Quan, R., Mendoza, I., Wu, Y., Du, W., Zhao, S., Schumaker, K. S., Pardo, J. M., & Guo, Y. (2009). Phosphorylation of SOS3-like calcium binding protein8 by SOS2 protein kinase stabilizes their protein complex and regulates salt tolerance in arabidopsis. *The Plant Cell*, *21*, 1607–1619.

Lux, A., Morita, S., Abe, J., & Ito, K. (2005). An improved method for clearing and staining free-hand sections and whole-mount samples. *Annals of Botany*, *96*, 989–996. https://doi.org/10.1093/aob/mci266

McCully, M. (1995). How do real roots work? Some new views of root structure. *Plant Physiology*, *109*, 1–6. https://doi.org/10.1104/pp.109.1.1

McCully, M. E. (1999). ROOTS IN SOIL: Unearthing the complexities of roots and their rhizospheres. *Annual Review of Plant Physiology and Plant Molecular Biology*, *50*, 695–718. https://doi.org/10.1146/annurev.arplant.50.1.695

Moghaieb, R. E. A., Sharaf, A. N., Soliman, M. H., El-Arabi, N. I., & Momtaz, O. A. (2014). An efficient and reproducible protocol for the production of salt tolerant transgenic wheat plants expressing the Arabidopsis AtNHX1 gene. *GM Crops Food*, *5*, 132–138.

Mohammadkhani, N., Heidari, R., Abbaspour, N., & Rahmani, F. (2016). Salinity effects on expression of some important genes in sensitive and tolerant grape genotypes. *Turkish Journal of Biology*, *40*, 95–108. https://doi.org/10.3906/biy-1501-67

Møller, I. S., Gilliham, M., Jha, D., Mayo, G. M., Roy, S. J., Coates, J. C., Haseloff, J., & Tester, M. (2009). Shoot $Na^+$ exclusion and increased salinity tolerance engineered by cell type - Specific alteration of Na+ transport in Arabidopsis. *The Plant Cell*, *21*, 2163–2178.

Munns, R., James, R. A., Gilliham, M., Flowers, T. J., & Colmer, T. D. (2016). Tissue tolerance: An essential but elusive trait for salt-tolerant crops. *Functional Plant Biology*, *43*, 1103–1113. https://doi.org/10.1071/FP16187

Munns, R., Passioura, J. B., Colmer, T. D., & Byrt, C. S. (2020). Osmotic adjustment and energy limitations to plant growth in saline soil. *New Phytologist*, *225*, 1091–1096. https://doi.org/10.1111/nph.15862

Naseer, S., Lee, Y., Lapierre, C., Franke, R., Nawrath, C., & Geldner, N. (2012). Casparian strip diffusion barrier in Arabidopsis is made of a lignin polymer without suberin. *Proceedings of the National Academy of Sciences of the United States of America*, *109*, 10101–10106. https://doi.org/10.1073/pnas.1205726109

Oh, D. H., Barkla, B. J., Vera-Estrella, R., Pantoja, O., Lee, S. Y., Bohnert, H. J., & Dassanayake, M. (2015). Cell type-specific responses to salinity - the epidermal bladder cell transcriptome of Mesembryanthemum crystallinum. *New Phytologist*, *207*, 627–644.

Park, M., Lee, H., Lee, J. S., Byun, M. O., & Kim, B. G. (2009). In planta measurements of $Na^+$ using fluorescent dye CoroNa Green. *Journal of Plant Biology*, *52*, 298–302. https://doi.org/10.1007/s12374-009-9036-8

Picchioni, G. A., Miyamoto, S., & Storey, J. B. (1990). Salt effects on growth and ion uptake of pistachio rootstock seedlings. *Journal of the American Society for Horticultural Science*, *115*, 647–653. https://doi.org/10.21273/JASHS.115.4.647

Pradhan Mitra, P., & Loqué, D. (2014). Histochemical staining of Arabidopsis thaliana secondary cell wall elements. *Journal of Visualized Experiments* (87), e51381. https://doi.org/10.3791/51381

R Core Team. (2017). *R: A language and environment for statistical computing*. R Foundation for Statistical Computing. https://www.r-project.org/

Rahneshan, Z., Nasibi, F., & Moghadam, A. A. (2018). Effects of salinity stress on some growth, physiological, biochemical parameters and nutrients in two pistachio (Pistacia vera L.) rootstocks. *Journal of Plant Interactions*, *13*, 73–82.

Ramirez-Flores, M. R., Rellan-Alvarez, R., Wozniak, B., Gebreselassie, M. N., Jakobsen, I., Olalde-Portugal, V., Baxter, I., Paszkowski, U., & Sawers, R. J. H. (2017). Co-ordinated changes in the accumulation of metal ions in maize (Zea mays ssp. mays L.) in response to inoculation with the arbuscular mycorrhizal fungus funneliformis mosseae. *Plant and Cell Physiology*, *58*, 1689–1699. https://doi.org/10.1093/pcp/pcx100

Ranathunge, K., Schreiber, L., & Franke, R. (2011). Suberin research in the genomics era-New interest for an old polymer. *Plant Science*, *180*, 399–413. https://doi.org/10.1016/j.plantsci.2010.11.003

Rewald, B., Raveh, E., Gendler, T., Ephrath, J. E., & Rachmilevitch, S. (2012). Phenotypic plasticity and water flux rates of Citrus root orders under salinity. *Journal of Experimental Botany*, *63*, 2717–2727. https://doi.org/10.1093/jxb/err457

Rosquete, M. R., Worden, N., Ren, G., Sinclair, R. M., Pfleger, S., Salemi, M., Phinney, B. S., Domozych, D., Wilkop, T., & Drakakaki, G. (2019). AtTRAPPC11/ROG2: A role for TRAPPs in maintenance of the plant trans-golgi network/early endosome organization and function. *The Plant Cell*, *31*, 1879–1898.

Rost, T. L. (2011). The organization of roots of dicotyledonous plants and the positions of control points. *Annals of Botany*, *107*, 1213–1222. https://doi.org/10.1093/aob/mcq229

Rubio, F., Gassmann, W., & Schroeder, J. I. (1995). Sodium-driven potassium uptake by the plant potassium transporter HKT1 and mutations conferring salt tolerance. *Science*, *270*, 1660–1663. https://doi.org/10.1126/science.270.5242.1660

Rui, Y., & Dinneny, J. R. (2020). A wall with integrity: Surveillance and maintenance of the plant cell wall under stress. *New Phytologist*, *225*, 1428–1439. https://doi.org/10.1111/nph.16166

Ruiz, M., Quiñones, A., Martínez-Cuenca, M. R., Aleza, P., Morillon, R., Navarro, L., Primo-Millo, E., & Martínez-Alcántara, B. (2016). Tetraploidy enhances the ability to exclude chloride from leaves in carrizo citrange seedlings. *Journal of Plant Physiology*, *205*, 1–10. https://doi.org/10.1016/j.jplph.2016.08.002

Salas-González, I., Reyt, G., Flis, P., Custódio, V., Gopaulchan, D., Bakhoum, N., Dew, T. P., Suresh, K., Franke, R. B., Dangl, J. L., & Salt, D. E. (2020). Coordination between microbiota and root endodermis supports plant mineral nutrient homeostasis. *Science*, *371*, eabd0695.

Schneider, C. A., Rasband, W. S., & Eliceiri, K. W. (2012). NIH Image to ImageJ: 25 years of image analysis. *Nature Methods*, *9*, 671–675. https://doi.org/10.1038/nmeth.2089

Serra, O., Soler, M., Hohn, C., Sauveplane, V., Pinot, F., Franke, R., Schreiber, L., Prat, S., Molinas, M., & Figueras, M. (2009). CYP86A33-targeted

gene silencing in potato tuber alters suberin composition, distorts suberin lamellae, and impairs the periderm's water barrier function. *Plant Physiology*, *149*, 1050–1060.

Shabala, L., Cuin, T. A., Newman, I. A., & Shabala, S. (2005). Salinity-induced ion flux patterns from the excised roots of Arabidopsis sos mutants. *Planta*, *222*, 1041–1050. https://doi.org/10.1007/s00425-005-0074-2

Shao, Y., Cheng, Y., Pang, H., Chang, M., He, F., Wang, M., Davis, D. J., Zhang, S., Betz, O., Fleck, C., Dai, T., Madahhosseini, S., Wilkop, T., Jernstedt, J., & Drakakaki, G. (2021). Investigation of salt tolerance mechanisms across a root developmental gradient in almond rootstocks. *Frontiers in Plant Science* (11), 595055. https://doi.org/10.3389/fpls.2020.595055

Shen, J., Xu, G., & Zheng, H. Q. (2015). Apoplastic barrier development and water transport in Zea mays seedling roots under salt and osmotic stresses. *Protoplasma*, *252*, 173–180. https://doi.org/10.1007/s00709-014-0669-1

Shi, H., Ishitani, M., Kim, C., & Zhu, J. K. (2000). The Arabidopsis thaliana salt tolerance gene SOS1 encodes a putative $Na^+/H^+$ antiporter. *Proceedings of the National Academy of Sciences of the United States of America*, *97*, 6896–6901. https://doi.org/10.1073/pnas.120170197

Shi, H., Lee, B.-H., Wu, S.-J., & Zhu, J.-K. (2003). Overexpression of a plasma membrane $Na^+/H^+$ antiporter gene improves salt tolerance in Arabidopsis thaliana. *Nature Biotechnology*, *21*, 81–85. https://doi.org/10.1038/nbt766

Shohan, M. U. S., Sinha, S., Nabila, F. H., Dastidar, S. G., & Seraj, Z. I. (2019). HKT1;5 transporter gene expression and association of amino acid substitutions with salt tolerance across rice genotypes. *Frontiers in Plant Science*, *10*, 1–18. https://doi.org/10.3389/fpls.2019.01420

Storey, R., & Walker, R. R. (1998). Citrus and salinity. *Scientia Horticulturae*, *78*, 39–81. https://doi.org/10.1016/S0304-4238(98)00190-3

Tataranni, G., Santarcangelo, M., Sofo, A., Xiloyannis, C., Tyerman, S. D., & Dichio, B. (2015). Correlations between morpho-anatomical changes and radial hydraulic conductivity in roots of olive trees under water deficit and rewatering. *Tree Physiology*, *35*, 1356–1365. https://doi.org/10.1093/treephys/tpv074

Tester, M., & Davenport, R. (2003). $Na^+$ tolerance and $Na^+$ transport in higher plants. *Annals of Botany*, *91*, 503–527. https://doi.org/10.1093/aob/mcg058

Tyerman, S. D., Munns, R., Fricke, W., Arsova, B., Barkla, B. J., Bose, J., Bramley, H., Byrt, C., Chen, Z., Colmer, T. D., Cuin, T., Day, D. A., Foster, K. J., Gilliham, M., Henderson, S. W., Horie, T., Jenkins, C. L. D., Kaiser, B. N., Katsuhara, M., … Wen, Z. (2019). Energy costs of salinity tolerance in crop plants. *New Phytologist*, *221*, 25–29. https://doi.org/10.1111/nph.15555

van Zelm, E., Zhang, Y., & Testerink, C. (2020). Salt tolerance mechanisms of plants. *Annual Review of Plant Biology*, *71*, 403–433. https://doi.org/10.1146/annurev-arplant-050718-100005

Vishal, B., Krishnamurthy, P., Ramamoorthy, R., & Kumar, P. P. (2019). OsTPS8 controls yield-related traits and confers salt stress tolerance in rice by enhancing suberin deposition. *New Phytologist*, *221*, 1369–1386.

Volkov, V., Wang, B., Dominy, P. J., Fricke, W., & Amtmann, A. (2004). Thellungiella halophila, a salt-tolerant relative of Arabidopsis thaliana, possesses effective mechanisms to discriminate between potassium and sodium. *Plant, Cell and Environment*, *27*, 1–14. https://doi.org/10.1046/j.0016-8025.2003.01116.x

Wachsman, G., Sparks, E., & Benfey, P. N. (2015). Genes and networks regulating root anatomy and architecture Tansley review Genes and networks regulating root anatomy and architecture. 26–38.

Walker, R. R., Torokfalvy, E., & Behboudian, M. H. (1987). Uptake and distribution of chloride, sodium and potassium ions and growth of salt-treated pistachio plants. *Australian Journal of Agricultural Research*, *38*, 383–394. https://doi.org/10.1071/AR9870383

Wang, P., Wang, C.-M., Gao, L. I., Cui, Y.-N., Yang, H.-L., de Silva, N. D. G., Ma, Q., Bao, A.-K., Flowers, T. J., Rowland, O., & Wang, S.-M. (2020). Aliphatic suberin confers salt tolerance to Arabidopsis by limiting $Na^+$ influx, $K^+$ efflux and water backflow. *Plant and Soil*, *448*, 603–620. https://doi.org/10.1007/s11104-020-04464-w

Wu, H., Shabala, L., Liu, X., Azzarello, E., Zhou, M., Pandolfi, C., Chen, Z. H., Bose, J., Mancuso, S., & Shabala, S. (2015). Linking salinity stress tolerance with tissue-specific $Na^+$ sequestration in wheat roots. *Frontiers in Plant Science*, *6*, 1–13. https://doi.org/10.3389/fpls.2015.00071

Wu, H., Shabala, L., Zhou, M., Su, N., Wu, Q., Ul-Haq, T., Zhu, J., Mancuso, S., Azzarello, E., & Shabala, S. (2019). Root vacuolar Na+ sequestration but not exclusion from uptake correlates with barley salt tolerance. *The Plant Journal*, *100*, 55–67.

Yang, Q., Chen, Z. Z., Zhou, X. F., Yin, H. B., Li, X., Xin, X. F., Hong, X. H., Zhu, J. K., & Gong, Z. (2009). Overexpression of SOS (salt overly sensitive) genes increases salt tolerance in transgenic Arabidopsis. *Molecular Plant*, *2*, 22–31. https://doi.org/10.1093/mp/ssn058

Yang, Y., & Guo, Y. (2018). Elucidating the molecular mechanisms mediating plant salt-stress responses. *New Phytologist*, *217*, 523–539. https://doi.org/10.1111/nph.14920

Yeo, A. R., Flowers, S. A., Rao, G., Welfare, K., Senanayake, N., & Flowers, T. J. (1999). Silicon reduces sodium uptake in rice (Oryza sativa L.) in saline conditions and this is accounted for by a reduction in the transpirational bypass flow. *Plant, Cell and Environment*, *22*, 559–565.

Zeng, Y., Li, Q., Wang, H., Zhang, J., Du, J., Feng, H., Blumwald, E., Yu, L., & Xu, G. (2018). Two NHX-type transporters from Helianthus tuberosus improve the tolerance of rice to salinity and nutrient deficiency stress. *Plant Biotechnology Journal*, *16*, 310–321.

Zhang, H. X., & Blumwald, E. (2001). Transgenic salt-tolerant tomato plants accumulate salt in foliage but not in fruit. *Nature Biotechnology*, *19*, 765–768. https://doi.org/10.1038/90824

Zhang, J., Wang, L., Liu, Y., Li, D., Feng, S., Yang, J., Zhang, J., Wang, D., & Gan, Y. (2019). Improving salt tolerance in potato through overexpression of AtHKT1 gene. *BMC Plant Biology*, *19*, 1–15.

Zhu, J. K. (2002). Salt and drought stress signal transduction in plants. *Annual Review of Plant Biology*, *53*, 247–273.

Zohary, D., & Spiegl-Roy, P. (1975). Beginning of fruit growing in the old world. *Science*, *87*, 319–327.

Zolla, G., Heimer, Y. M., & Barak, S. (2010). Mild salinity stimulates a stress-induced morphogenic response in Arabidopsis thaliana roots. *Journal of Experimental Botany*, *61*, 211–224. https://doi.org/10.1093/jxb/erp290

## SUPPORTING INFORMATION

Additional Supporting Information may be found online in the Supporting Information section.

**How to cite this article:** Zhang S, Quartararo A, Betz OK, et al. Root vacuolar sequestration and suberization are prominent responses of *Pistacia* spp. rootstocks during salinity stress. *Plant Direct*. 2021;5:e00315. https://doi.org/10.1002/pld3.315